Scaling behaviour of the thermopower in a two-component composite near a percolation threshold

1992 J. Phys. A: Math. Gen. 25 1875

(http://iopscience.iop.org/0305-4470/25/7/027)

J. Phys. A: Math. Gen. 25 (1992) 1875–1884. Printed in the UK

Scaling behaviour of the thermopower in a two-component composite near a percolation threshold

Ohad Levy and David J Bergman

School of Physics and Astronomy, Raymond and Beverly Sackler Faculty of Exact Sciences, Tel Aviv University, Tel Aviv 69978, Israel

Received 28 August 1991

Abstract. An exact relation between the bulk effective Seebeck coefficient α_e of a composite conductor and the bulk effective electrical and thermal conductivities σ_e and γ_e is used to study the scaling behaviour of α_e near percolation. The behaviour turns out to be quite rich, as a result of its dependence on three dimensionless small parameters, namely, the electrical and thermal conductivity ratios of the two components σ_I/σ_M, γ_I/γ_M, and the distance away from the percolation threshold $\Delta p \equiv p_M - p_c$. The behaviour of the thermoelectric figure of merit Z_e in the different parts of the critical region is also discussed.

1. Introduction

The thermoelectric effect is perhaps the simplest type of coupled field transport known in solids. Other types include magneto-transport, the study of which in percolating media has already yielded some interesting qualitative as well as quantitative results [1–4]. In this article we report on a theoretical study we have made of the critical behaviour of the thermoelectric properties of a two-component percolative medium. In order to do this, we exploit a field decoupling transformation which, when applied to the thermoelectric transport problem in a two-component composite, transforms it into a pair of uncoupled, simple conductivity-like transport problems in the same composite. This transformation, discovered by Straley [5], was already used by him to calculate the thermopower of a two-component composite. However the scaling behaviour near percolation is not discussed in that article. The results reported are largely numerical or graphical, and are confined to one particular category of components, which is the common one. Here we take up where [5] left off, and study other categories of components. We also use the scaling description of critical behaviour in simple, one-field conductivity, in order to work out explicitly the leading forms of the critical behaviour for the Seebeck coefficient in various sectors of the critical region. The fact that there are many such sectors with qualitatively different forms of behaviour is due to the appearance of three critical parameters in the problem, namely, the electrical conductivity ratio σ_I/σ_M, the thermal conductivity ratio γ_I/γ_M and the volume fraction difference $\Delta p \equiv p_M - p_c$, where the subscripts M, I refer to the good and the bad conductor, respectively, and p_c is the good conductor percolation threshold. Because of this, even when all three parameters are small, there are six different asymptotic sectors in the critical region, corresponding to six different permutations or orderings by size of these parameters. The corresponding richness of different possible critical behaviours is reminiscent of the similar richness that was found, both

0305-4470/92/071875+10$04.50

theoretically [3], and experimentally [4], in the critical behaviour of the low field Hall effect near a percolation threshold. In analogy with those results, we have found that in a good conductor–bad conductor mixture, the thermoelectric effect can, in some cases, be dominated by the good conductor even below its percolation threshold and, in some other cases, be dominated by the bad conductor even above that threshold.

The rest of this article is organized as follows. In section 2 we introduce our notation and summarize the theory of thermoelectricity in two-component composites, as well as the scaling description of simple, one-field conductivity near a percolation threshold. In section 3 we apply these elements to a discussion of the critical behaviour of the Seebeck coefficient and of the thermoelectric quality factor near a percolation threshold.

2. Theoretical framework

The electric current density that flows in a homogeneous material due to electric and temperature fields under linear response assumptions is given by

$$\boldsymbol{J}_E = -\sigma\nabla\Phi - \sigma\alpha\nabla T \tag{1}$$

where Φ is the electric potential, T is the temperature, σ is the electrical conductivity and α is the thermoelectric coefficient or Seebeck coefficient. The entropy current density under the same conditions is given by

$$\boldsymbol{J}_S = -\sigma\alpha\nabla\Phi - \frac{\gamma}{T}\nabla T \tag{2}$$

where γ is the thermal conductivity at zero electric field. These equations can be summarized in the following compact form

$$\mathbf{J} = \mathbf{S}\nabla\Phi \tag{3}$$

where

$$\mathbf{J} \equiv \begin{pmatrix} -\boldsymbol{J}_E/e \\ -\boldsymbol{J}_S/k \end{pmatrix} \qquad \Phi \equiv \begin{pmatrix} \nabla(e\Phi) \\ \nabla(kT) \end{pmatrix} \qquad \mathbf{S} \equiv \begin{pmatrix} \sigma/e^2 & \sigma\alpha/ek \\ \sigma\alpha/ek & \gamma/k^2T \end{pmatrix}. \tag{4}$$

The absolute charge of the electron e and Boltzmann's constant k have been included in these definitions in order to make both elements of Φ have the same physical dimensions, and likewise for the elements of $\mathbf{J}$ and of the thermoelectric transport matrix $\mathbf{S}$. The thermoelectric figure of merit is defined by

$$Z \equiv \left(\frac{\gamma}{\sigma\alpha^2} - T\right)^{-1}. \tag{5}$$

It determines the maximum efficiency of a thermoelectric heat pump constructed from this material [6].

Each component material of an inhomogeneous composite is characterized by its own transport matrix $\mathbf{S}_a$. The material as a whole is then characterized by an effective transport matrix

$$\mathbf{S}_e = \begin{pmatrix} \sigma_e/e^2 & \sigma_e\alpha_e/ek \\ \sigma_e\alpha_e/ek & \gamma_e/k^2T \end{pmatrix} \tag{6}$$

which relates the volume averaged fluxes $\langle\mathbf{J}\rangle$ to the volume averaged fields $\langle\nabla\Phi\rangle$

$$\langle\mathbf{J}\rangle = \mathbf{S}_e\langle\nabla\Phi\rangle. \tag{7}$$

Note that although we assume that the components are isotropic, we do not assume this for the composite: In the case of an anisotropic composite, our notation assumes that both of the volume averaged fields $\langle \nabla \Phi \rangle$, $\langle \nabla T \rangle$ point along the same direction, say along the x-axis, and that only the x-component of the volume averaged currents $\langle \boldsymbol{J}_E \rangle$, $\langle \boldsymbol{J}_S \rangle$ are determined by the 2×2 matrix $\mathbf{S}_e$.

In order to find useful forms for the bulk effective moduli σ_e, γ_e and α_e we use a diagonalization method similar to the one first suggested by Straley [5] and later generalized by Milgrom and Shtrikman [7]: We find a real symmetric matrix

$$\mathbf{d} = \begin{pmatrix} d_{11} & d_{12} \\ d_{12} & d_{22} \end{pmatrix} \tag{8}$$

such that $\mathbf{d}\mathbf{S}_a\mathbf{d}$ is diagonal for both components $a = A, B$. Explicit expressions can easily be found for the elements of the transformation matrix $\mathbf{d}$ in terms of the elements of $\mathbf{S}_A$ and $\mathbf{S}_B$ [8]. Having thus transformed the coupled-field transport problem into a pair of uncoupled, simple conductivity-like transport problems, we can describe the uncoupled transport in the composite medium by a bulk effective diagonal matrix $\mathbf{S}'_e$

$$\mathbf{S}'_e = \begin{pmatrix} S'_{e11} & 0 \\ 0 & S'_{e22} \end{pmatrix}. \tag{9}$$

The bulk effective matrix $\mathbf{S}_e$ for the original, coupled field transport problem can now be obtained from $\mathbf{S}'_e$ by the inverse transformation $\mathbf{S}_e = \mathbf{d}^{-1}\mathbf{S}'_e\mathbf{d}^{-1}$. When this is used to calculate the effective moduli of the composite we find

$$\sigma_e = e^2 \frac{d_{22}^2 S'_{e11} + d_{12}^2 S'_{e22}}{(d_{11}d_{22} - d_{12}^2)^2} \tag{10}$$

$$\gamma_e = k^2 T \frac{d_{12}^2 S'_{e11} + d_{11}^2 S'_{e22}}{(d_{11}d_{22} - d_{12}^2)^2} \tag{11}$$

$$\alpha_e = -\frac{k}{e}\frac{d_{12}}{d_{22}}\left(1 + \frac{d_{11}d_{22} - d_{12}^2}{d_{12}^2 + d_{22}^2 S'_{e11}/S'_{e22}}\right). \tag{12}$$

The fact that σ_e, γ_e and α_e all depend on the same two quantities S'_{e11} and S'_{e22} can be used to derive an exact relation among them [7, 8]:

$$\frac{\alpha_B - \alpha_e}{\alpha_B - \alpha_A} = \frac{\dfrac{\gamma_e}{\gamma_B}\Big/\dfrac{\sigma_e}{\sigma_B} - 1}{\dfrac{\gamma_A}{\gamma_B}\Big/\dfrac{\sigma_A}{\sigma_B} - 1}. \tag{13}$$

Note, however, that σ_e depends on all six of the component parameters $\sigma_A, \sigma_B, \gamma_A, \gamma_B, \alpha_A, \alpha_B$ and not merely on the pair of electrical conductivities σ_A, σ_B, as would be the case in the absence of thermoelectricity, when all the α's vanish. A similar statement holds for γ_e. The effective figure of merit is now given by [8]

$$Z_e = \left(\frac{\gamma_e}{\sigma_e \alpha_e^2} - T\right)^{-1} = \frac{1}{T}\frac{\left(\dfrac{S'_{e11}}{S'_{e22}} + \dfrac{d_{11}}{d_{22}}\right)^2}{\dfrac{S'_{e11}}{S'_{e22}}\left(\dfrac{d_{12}}{d_{22}} - \dfrac{d_{11}}{d_{12}}\right)^2}. \tag{14}$$

Since α_e as well as Z_e depend upon the single ratio S'_{e11}/S'_{e22}, the critical behaviour is also entirely determined by this ratio. The quantities S'_{e11}, S'_{e22} are the bulk effective

conductivities of two uncoupled conductivity problems in two composites with the same microgeometry but different components. We can, therefore, write

$$\frac{S'_{eii}}{S'_{Mii}} = m\left(\frac{S'_{Iii}}{S'_{Mii}}\right) \qquad \text{for } i = 1, 2 \tag{15}$$

where the detailed form of the function $m(h)$ depends on the precise microgeometry. In the vicinity of the percolation threshold, i.e. where both h and $\Delta p \equiv p_M - p_c$ are small, this function has a scaling form [9]

$$m(h, \Delta p) = |\Delta p|^t \mathcal{F}\left(\frac{h}{|\Delta p|^{t+s}}\right) \tag{16}$$

where $\mathcal{F}(z)$ has the following asymptotic forms

$$\mathcal{F}(z) \sim \begin{cases} \text{constant} & \Delta p < 0\text{: } z \ll 1 \qquad \text{regime I} \\ z & \Delta p < 0\text{; } z \ll 1 \qquad \text{regime II} \\ z^{(t/(t+s))} & z \gg 1 \qquad \text{regime III.} \end{cases} \tag{17}$$

These asymptotic forms will suffice for discussing the different asymptotic regimes of the thermoelectric behaviour. However, when one is interested in the thermoelectric behaviour throughout the critical region, one needs the explicit form of the scaling function $\mathcal{F}(z)$ for all values of z. For that purpose we shall use the parametric form suggested and used earlier by Straley [10]

$$\mathcal{F} = \lambda^t(1+x) \qquad \lambda x = \Delta p \qquad z = \lambda^{s+t}(1-x^2). \tag{18}$$

Here t and s are the conductivity critical exponents, which in three-dimensional percolation have the universal values $t \simeq 2.0$ [11] and $s \simeq 0.75$ [12].

3. Scaling behaviour near percolation

In our study we always assumed that σ_I/σ_M, γ_I/γ_M and $|\Delta p|$ are all small compared to unity. We then fixed the two ratios and allowed $|\Delta p|$ to vary. The critical behaviour of the bulk effective thermoelectric moduli of the composite was studied numerically, using expressions (12), (14) and (18). The behaviour of α_e was also studied analytically for the limit of very small Seebeck coefficients in both components, which is the common case in practice, using expressions (13) and (17).

3.1. Numerical results

Typical results for the critical behaviour of α_e are shown in figure 1. We see three different types of behaviour depending on the electrical conductivities ratio and the thermal conductivities ratio of the components. One type of behaviour appears when $\sigma_I/\sigma_M \ll \gamma_I/\gamma_M \ll 1$ (the common case in practice). Then, if we decrease p_M starting above p_c, the effective thermopower increases very slowly at first, staying very close to α_M. At p_c, and even slightly below it, it is still nearly equal to the pure good conductor value α_M. Below p_c the effective thermopower increases abruptly, levelling off to the bad conductor value α_I only a considerable distance below p_c. In the other case $\gamma_I/\gamma_M \ll \sigma_I/\sigma_M \ll 1$, which is much less common in practice, a similar sequence of events is found to occur when p_M *increases* through p_c (see figure 1): At first α_e

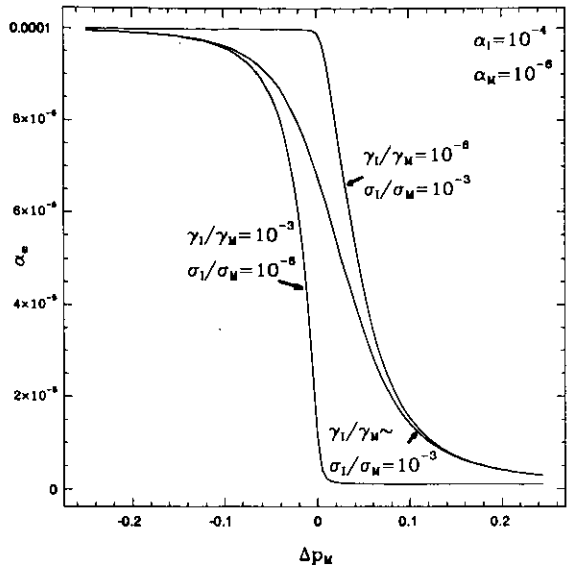

Figure 1. The effective Seebeck coefficient α_e of a good conductor–bad conductor composite versus the good conductor concentration p_M, for different values of the thermal and electrical conductivity ratios.

remains very close to α_I, then an abrupt decrease occurs above p_c, while levelling out to α_M takes place only when p_M is considerably above p_c. Finally, when the two conductivity ratios have *similar* magnitudes, the transition at percolation, from α_M to α_I, is almost symmetric about p_c (see figure 1). These qualitative features do not depend on the precise values of the Seebeck coefficients of the components. However, the *detailed shape* of the transition in the first case (the common one) *does* depend on the value of the thermoelectric coefficient of the good conductor, as shown in figure 2: As α_M increases and approaches its maximum allowed value of $\sqrt{\gamma_M/(\sigma_M T)}$, the transition becomes less abrupt. For values of α_M very close to this limit the transition is so slow that it is obvious it cannot describe the real behaviour outside of a very small region below p_c. For comparison, we calculated the critical behaviour for these cases using Bruggeman's symmetric effective medium approximation for the uncoupled effective conductivities S'_{e11} and S'_{e22} [13]. This calculation should give good results for small volume fractions of the good conductor, far below p_c. These results are shown in figure 3. Comparing figures 2 and 3 it is apparent that for small α_M (i.e. far from its upper limit) the scaling calculation gives good results in a large range below p_c, whereas for values of α_M that are close to the upper limit, the behaviour far below p_c changes considerably and the result of the scaling approximation is not valid. Such changes in the critical behaviour with variations of either α_M or α_I do not arise in the opposite case, when α_e is dominated by the bad conductor.

The effective thermoelectric figure of merit Z_e can be similarly calculated. Unlike α_e, Z_e is not always a monotonic function of the ratio S'_{e11}/S'_{e22}. It has a single minimum when $S'_{e11}/S'_{e22} = |d_{11}/d_{22}|$, if that value is inside the range of allowed values [8]. Therefore, if $|d_{11}/d_{22}|$ lies between the pure component values of S'_{e11}/S'_{e22}, this minimum is attained when p_M is varied, otherwise the minimum is not attained and the transition is monotonic. The condition for the attainability of this minimum,

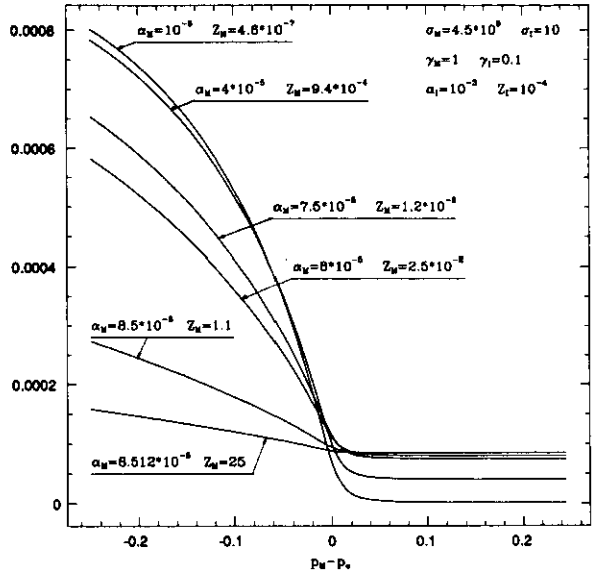

Figure 2. The effective Seebeck coefficient α_e for several values of α_M, up to the upper limit $\alpha_M = 8.513 \times 10^{-5}$, versus the good conductor concentration p_M.

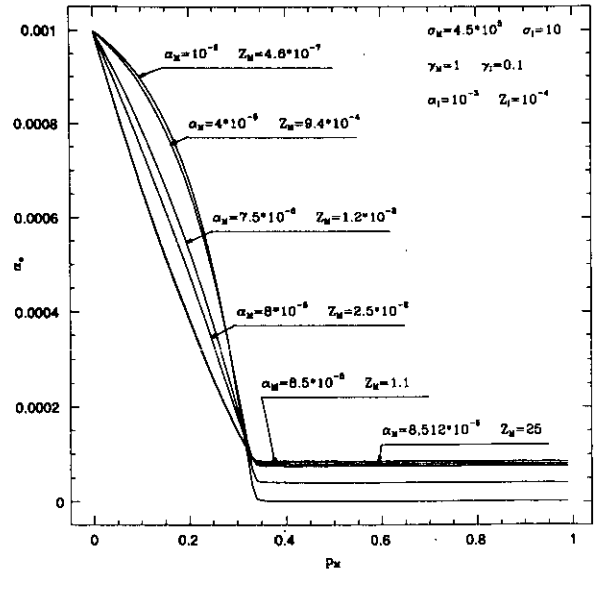

Figure 3. The same as figure 2, but using the effective medium approximation.

expressed in terms of the properties of the components is [14]:

$$\frac{\dfrac{\gamma_M}{\sigma_M}\alpha_I - \dfrac{\gamma_I}{\sigma_I}\alpha_M}{\alpha_M - \alpha_I} > 0. \tag{19}$$

Results of the scaling calculation of Z_e for the same cases as shown in figure 1 are shown in figure 4. The behaviour is found, again, to depend on the relation between

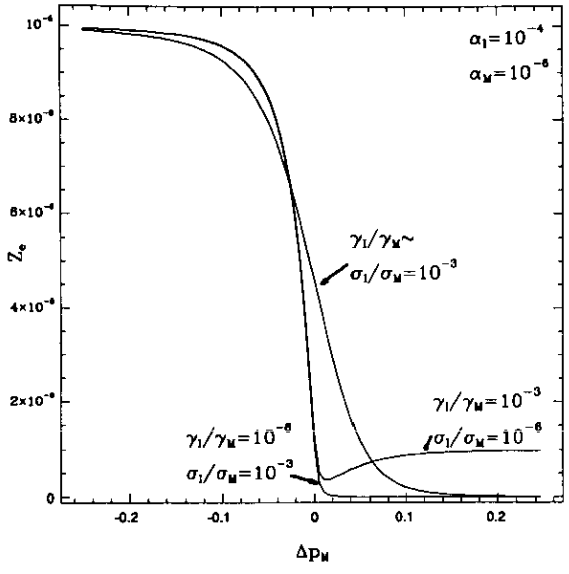

Figure 4. The effective figure of merit Z_e of a good conductor-bad conductor composite versus the good conductor concentration p_M, for the same cases as figure 1, using the scaling function of equation (18).

the thermal conductivities ratio γ_I/γ_M and the electrical conductivities ratio σ_I/σ_M. When the two ratios are similar the transition at percolation, from Z_M to Z_I, is almost symmetric about p_c. If $\gamma_I/\gamma_M \ll \sigma_I/\sigma_M \ll 1$, then Z_e still changes monotonically with Δp from the good conductor value Z_M to the bad conductor value Z_I, but the transition is no longer symmetric about p_c. At the threshold, Z_e is much smaller than in the first case. In the other case $\sigma_I/\sigma_M \ll \gamma_I/\gamma_M \ll 1$, and when the condition (19) is also satisfied (this is the common case in practice), Z_e is non-monotonic and has a minimum slightly above p_c. The location of the minimum is determined by the pure component values of Z. As Z_M increases the minimum moves to smaller values of p_M, and may even cross to the other side of the percolation threshold p_c. A graph similar to our figures 1 and 4 for a particular case of the common type only was calculated and plotted by Straley [5].

The same calculations can be made starting from (13) and using (18) for the effective conductivities σ_e and γ_e. However, the results of such a calculation will be less accurate than those of the previous one, since σ_e and γ_e are not the uncoupled conductivities for which (18) is strictly valid. In order for this procedure to be a good approximation, the off-diagonal elements of the matrix S of (3) must be small compared to the diagonal elements. This is usually true in practice for each component and, consequently, also for the composite. The results of this calculation are then very similar to those of the previous, more exact one. The behaviour of the effective thermoelectric properties exhibits the same general features in each of the cases described above.

3.2. Analytic results

In order to analyse the different possible modes of behaviour analytically, we shall assume the common situation where $S_{12} \ll S_{11}$ and $S_{12} \ll S_{22}$ in both components. In that case γ_e/γ_M depends only on γ_I/γ_M while σ_e/σ_M depends only on σ_I/σ_M. Under

these conditions we can use the asymptotic scaling forms of (17) directly for the effective conductivities σ_e and γ_e, and then calculate α_e using (13).

The critical behaviour of the thermoelectric coefficient turns out to be quite rich since it depends on three small dimensionless parameters σ_I/σ_M, γ_I/γ_M and Δp, instead of just two parameters as in the familiar case of simple conductivity. This behaviour is again found to depend on the relation between the electrical and thermal conductivity ratios.

In the case that they are similar we find, above p_c

$$\frac{\alpha_M-\alpha_e}{\alpha_M-\alpha_I}\propto\left(\frac{\sigma_I}{\sigma_M}\right)(\Delta p)^{-t-s} \qquad \text{for } \frac{\sigma_I}{\sigma_M}\ll(\Delta p)^{t+s} \tag{20}$$

while below p_c we find $\alpha_e\approx\alpha_I$. In order to see the deviations from this value below p_c, we must consider the second term in the power series expansion of the scaling function $\mathcal{F}(z)=z+z^2+\ldots$. (Here and in subsequent expressions we ignore coefficients of the power series—they are expected to be of order 1.) We thus find

$$\frac{\alpha_M-\alpha_e}{\alpha_M-\alpha_I}\simeq 1-\left(\frac{\sigma_I}{\sigma_M}\right)|\Delta p|^{-t-s} \qquad \text{for } \frac{\sigma_I}{\sigma_M}\ll(\Delta p)^{t+s}. \tag{21}$$

At p_c, or very near to it, we find

$$\frac{\alpha_M-\alpha_e}{\alpha_M-\alpha_I}\propto\left(\frac{\gamma_I\sigma_M}{\sigma_I\gamma_M}\right)^{-s/(t+s)} \qquad \text{for } \frac{\sigma_I}{\sigma_M}\gg(\Delta p)^{t+s}. \tag{22}$$

The behaviour in the two extreme cases is as follows:

($\mathcal{A}$) $\gamma_I/\gamma_M\gg\sigma_I/\sigma_M$

(*a*) For $p_M>p_c$ and $(\Delta p)^{t+s}>(\gamma_I/\gamma_M)$ we get, as in the previous case,

$$\frac{\sigma_M-\alpha_e}{\alpha_M-\alpha_I}\propto\left(\frac{\sigma_I}{\sigma_M}\right)(\Delta p)^{-t-s}\ll 1. \tag{23}$$

This means that α_e remains very close to α_M as Δp decreases.

(*b*) For $p_M>p_c$ in the transition region $(\sigma_I/\sigma_M)\ll(\Delta p)^{t+s}\ll(\gamma_I/\gamma_M)$ we find

$$\frac{\alpha_M-\alpha_e}{\alpha_M-\alpha_I}\propto\left(\frac{\gamma_M}{\gamma_I}\right)^{s/(t+s)}\left(\frac{\sigma_I}{\sigma_M}\right)(\Delta p)^{-t}\ll 1. \tag{24}$$

The slow increase continues, but with a different exponent t. The effective thermopower α_e is still nearly equal to α_M.

(*c*) At p_c we have

$$\frac{\alpha_M-\alpha_e}{\alpha_M-\alpha_I}\propto\left(\frac{\gamma_I\sigma_M}{\gamma_M\sigma_I}\right)^{-s/(t+s)}\ll 1. \tag{25}$$

This means that α_e is nearly equal to α_M even at threshold. It gets smaller with increasing contrast between the thermal conductivities ratio and the electric conductivities ratio.

(*d*) Below p_c, for $(\sigma_I/\sigma_M)\ll|\Delta p|^{t+s}\ll(\gamma_I/\gamma_M)$, we have

$$\frac{\alpha_M-\alpha_e}{\alpha_M-\alpha_I}\propto\left(\frac{\gamma_M}{\gamma_I}\right)^{s/(t+s)}|\Delta p|^{s}-\frac{\gamma_M\sigma_I}{\gamma_I\sigma_M}. \tag{26}$$

The slow increase continues with the exponent s. The right-hand side is still much smaller than unity so α_e is dominated by the good conductor value even below p_c.

(*e*) Further below p_c, when $|\Delta p|^{t+s} > (\gamma_I/\gamma_M)$, we find

$$\frac{\alpha_M - \alpha_e}{\alpha_M - \alpha_I} \simeq 1 - \frac{\sigma_I}{\sigma_M}|\Delta p|^{-t-s}. \tag{27}$$

Now the RHS is very close to unity so α_e is only slightly smaller than α_I. The transition between (*d*) and (*e*) is very sharp and cannot be discerned from this type of simple scaling approach.

($\mathcal{B}$) $\gamma_I/\gamma_M \ll \sigma_I/\sigma_M$

(*a*) For $p_M > p_c$ and $(\Delta p)^{t+s} > (\sigma_I/\sigma_M)$ we get, as before,

$$\frac{\alpha_M - \alpha_e}{\alpha_M - \alpha_I} \propto \left(\frac{\sigma_I}{\sigma_M}\right)(\Delta p)^{-t-s} \ll 1 \tag{28}$$

so that α_e is only slightly greater than α_M.

(*b*) Above p_c, for $(\gamma_I/\gamma_M) \ll (\Delta p)^{t+s} \ll (\sigma_I/\sigma_M)$, we find

$$\frac{\alpha_M - \alpha_e}{\alpha_M - \alpha_I} \simeq 1 - \left(\frac{\sigma_M}{\sigma_I}\right)^{t/(t+s)}(\Delta p)^t. \tag{29}$$

The RHS is almost unity so α_e is now close to its bad conductor value α_I already above p_c. Here the sharp transition occurs above p_c.

(*c*) At p_c, α_e is nearly equal to α_I. It gets closer to α_I with increasing contrast between γ_I/γ_M and σ_I/σ_M.

(*d*) For $p_M < p_c$ and $(\gamma_I/\gamma_M) \ll (\Delta p)^{t+s} \ll (\sigma_I/\sigma_M)$, we get

$$\frac{\sigma_M - \alpha_e}{\alpha_M - \alpha_I} \simeq 1 - \left(\frac{\gamma_I}{\gamma_M}\right)\left(\frac{\sigma_I}{\sigma_M}\right)^{-t/(t+s)}|\Delta p|^{-s} \tag{30}$$

so that α_e continues to rise towards α_I with the exponent s.

(*e*) For below p_c, when $|\Delta p|^{t+s} > (\sigma_I/\sigma_M)$, we get $\alpha_e = \alpha_I$.

These results agree well with the results of the numerical calculations described before. Analytic scaling calculations for Z_e produce less clear-cut results, although a considerable qualitative difference in behaviour between the extreme cases is apparent.

Acknowledgments

This research was supported, in part, by a grant from the US-Israel Binational Science Foundation.

References

[1] Bergman D J, Duering E and Murat M 1990 *J. Stat. Phys.* **58** 1; additional references, including experimental ones, can be found in this article

[2] Bergman D J 1987 *Phil. Mag.* **56** 983

[3] Bergman D J and Stroud D 1985 *Phys. Rev.* B **32** 6097

[4] Dai U, Palevski A and Deutscher G 1987 *Phys. Rev.* B **36** 790

[5] Straley J P 1981 *J. Phys. D: Appl. Phys.* **14** 2101

[6] Harman T C and Honig J M 1967 *Thermoelectric and Thermomagnetic Effects and Applications* (New York: McGraw-Hill)

[7] Milgrom M and Shtrikman S 1989 *Phys. Rev. Lett.* **62** 1979

[8] Bergman D J and Levy O 1991 *J. Appl. Phys.* **70** 6821

[9] Straley J P 1976 *J. Phys. C: Solid State Phys.* **9** 783
[10] Straley J P 1978 *Electrical Transport and Optical Properties of Inhomogeneous Media* (*AIP Conference Proceedings 40* 118) ed J C Garland and D B Tanner
[11] Derrida B, Stauffer D, Herrmann H J and Vannimenus J 1983 *J. Phys. Lett.* **44** 1701
[12] Herrmann H J, Derrida B and Vannimenus J 1984 *Phys. Rev.* B **30** 4080
[13] Landauer R 1978 *Electrical Transport and Optical Properties of Inhomogeneous Media* (*AIP Conference Proceedings 40* 2) ed J C Garland and D B Tanner
[14] Levy O 1990 MSc Thesis, Tel-Aviv University, unpublished